

1 Design of Mach-Zehnder Interferometer

2 SAIRAM SRI VATSAVAI,¹

3 ¹*Brookhaven National Lab, Long Island, Newyork, USA*

4 *ssrivatsa@bnl.gov

5 **Abstract:** This report explains the working principles of the Mach-Zehnder interferometer(MZI)
6 and discusses the various steps including simulations and analytical modeling for designing the
7 components and circuit of MZI.

8 1. Modelling and Simulation

9 1.1. Waveguide

10 The waveguide dimensions considered for the design are $220 \text{ nm} \times 500 \text{ nm}$ on a silicon-on-
11 insulator (SOI) platform. The first order TE and TM mode field profiles are shown in Figure
12 1(a) and (b), as observed in TE mode light is strongly confined inside the waveguide whereas
13 for TM mode is scattered into the substrate. In addition, Figure 2(a) and (b) illustrates the
14 wavelength dependence of effective index (n_{eff}) and group index (n_g), respectively, where
15 n_{eff} decreases at longer wavelengths due to reduced mode confinement and increased field
16 extension into the cladding, while n_g increases according to the relation $n_g = n_{eff} - \lambda \frac{dn_{eff}}{d\lambda}$
17 because of the combined effect of material and waveguide dispersion leading to a more negative
18 $dn_{eff}/d\lambda$ at higher wavelengths. To complement the Lumerical simulations, we developed a
19 compact analytical model by fitting the simulation data to second-order polynomial equations.
20 The wavelength-dependent effective index can be characterized using the following polynomial
21 expression:

$$n_{eff} = 2.44 - 1.13 * \lambda - 0.02 * \lambda^2 \quad (1)$$

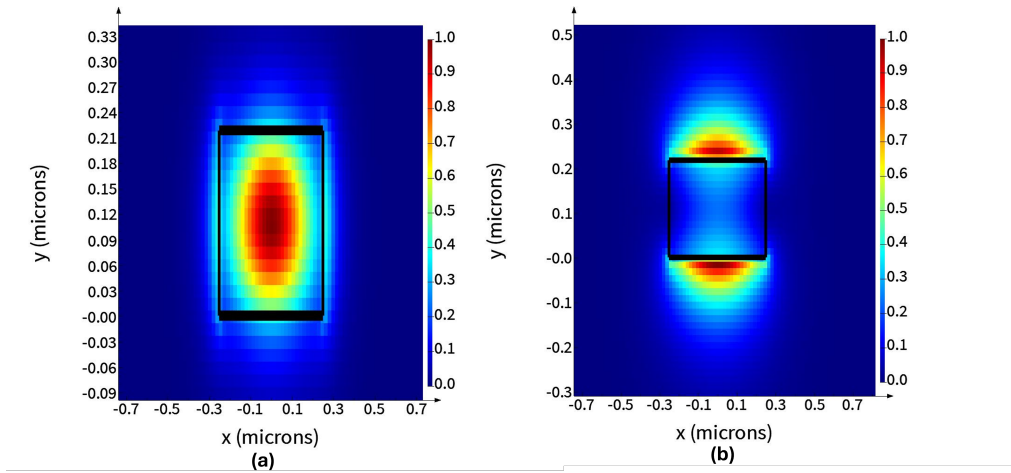


Fig. 1. Field profiles of waveguide (a) TE mode (b) TM mode.

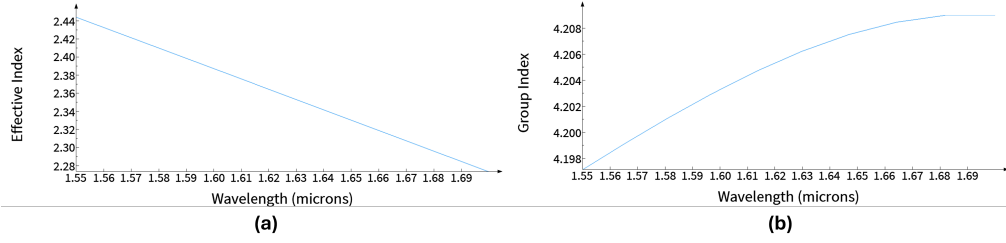


Fig. 2. (a) Effective index versus wavelength (b) Group indec versus wavelength.

22 1.2. MZI

23 In the layout, the MZIs are built using Y-branches and directional couplers. An MZI built using a
 24 Y-branch and a directional coupler consists of an initial Y-branch that splits the input signal into
 25 two arms, where a phase difference can be introduced, followed by a directional coupler that
 26 recombines the signals. The transfer function is given by:

$$I_{\text{out}} = I_{\text{in}} \left[\frac{1 + \cos(\Delta\phi)}{2} \right] \quad (2)$$

27 where $\Delta\phi$ is the phase difference between the arms, controlling the interference and output
 28 intensity.

29 The phase difference $\Delta\phi$ is introduced due to a path length difference ΔL between the two
 30 arms, it is given by:

$$\Delta\phi = \frac{2\pi}{\lambda} \cdot \Delta L \cdot n_{\text{eff}} \quad (3)$$

31 2. Layout

32 The layout is shown in Figure 3. It consists of two waveguides, each $150 \mu\text{m}$ in length. However,
 33 WG1 supports the TE mode, while WG2 supports the TM mode. In addition to the waveguides,
 34 four MZIs and an add drop MRR are included the layout. All devices are designed to operate in
 35 TE mode. The MZI1, MZI2, and MZI3 are designed with different path lengths. MZI4 is an
 36 exact replica of MZI3. Table 1 lists the individual path lengths of devices and their corresponding
 37 FSRs. The path lengths are determined to observe the change in FSR with respect to the path
 38 length. The MZI4 is designed to note the impact of fabrication variations. An add-drop microring
 39 resonator of $10 \mu\text{m}$ radius is added to verify the relationship between FSR and radius.

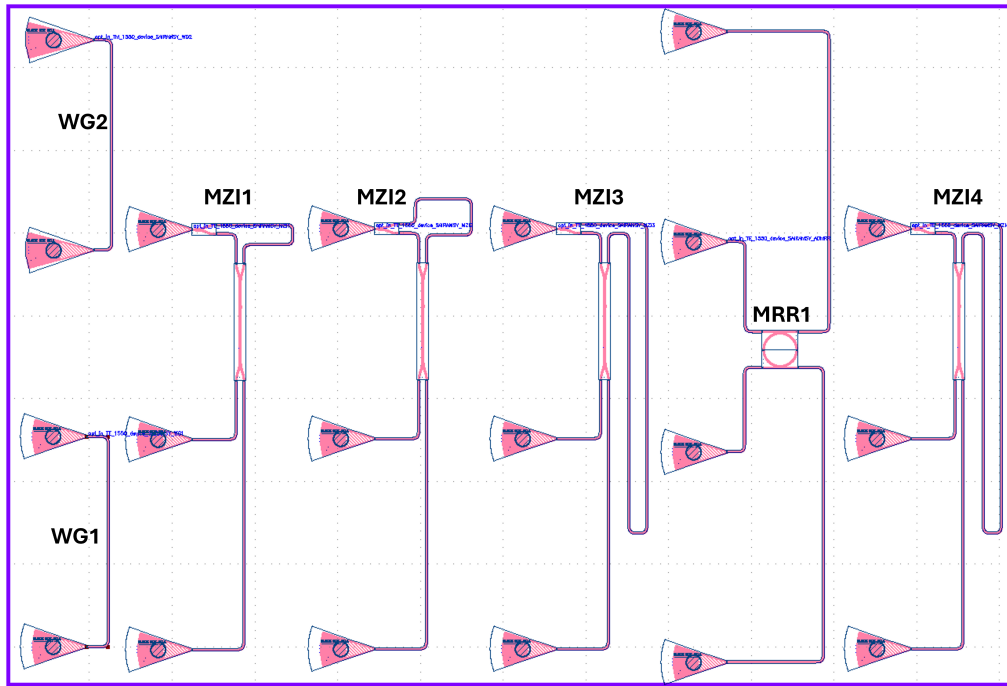


Fig. 3. Layout

Table 1. MZI Design Parameters

	MZI1		MZI2		MZI3		MZI4	
	l1	l2	l1	l2	l1	l2	l1	l2
Waveguide Length (μm)	28.14	94.5	28.14	116.76	28.14	440.6	28.14	440.6
ΔL (μm)	66.36		88.62		412.46		412.46	
Simulated FSR (nm)	8.67		6.48		1.4		1.4	
Measured FSR (nm)	8.7		6.45		1.38		1.4	

40 3. Corner Analysis

41 To understand manufacturing challenges and analyze the impact of manufacturing variations in
 42 the waveguide dimensions, we performed corner analysis. Table 2 shows the four corners and
 43 their corresponding waveguide dimensions. Using Lumerical Mode and matlab scripts, the group
 44 index and compact modelling parameters of the waveguides are reported. Further, using these
 45 corner analysis, we predict the variability in the circuit performance and report it in Table 3.

Table 2. Corner Analysis Waveguides

Corner	height(nm)	width(nm)	n1	n2	n3	ng
C1	223.1	510	2.46	-1.09	-0.036	4.17
C2	223.1	470	2.4	-1.187	-0.034	4.241
C3	215.3	470	2.36	-1.198	-0.0117	4.225
C4	215.3	510	2.43	-1.1	-0.02	4.156
nominal	220	500	2.44	-1.12	-0.03	4.175

Table 3. Corner Analysis MZI

Corner	MZI1		MZI2		MZI3		MZI4	
	FSR(nm)	ng_av	FSR(nm)	ng_av	FSR(nm)	ng_av	FSR(nm)	ng_av
C1	8.72	4.15	6.5	4.17	1.42	4.1	1.42	4.1
C2	5.83	4.24	6.39	4.24	1.39	4.19	1.39	4.19
C3	8.6	4.2	6.44	4.2	1.4	4.16	1.4	4.16
C4	8.73	4.14	6.52	4.15	1.43	4.07	1.43	4.07
Nominal	8.67		6.48		1.4		1.4	

46 **4. Measurement**

47 **4.1. Baseline Correction**

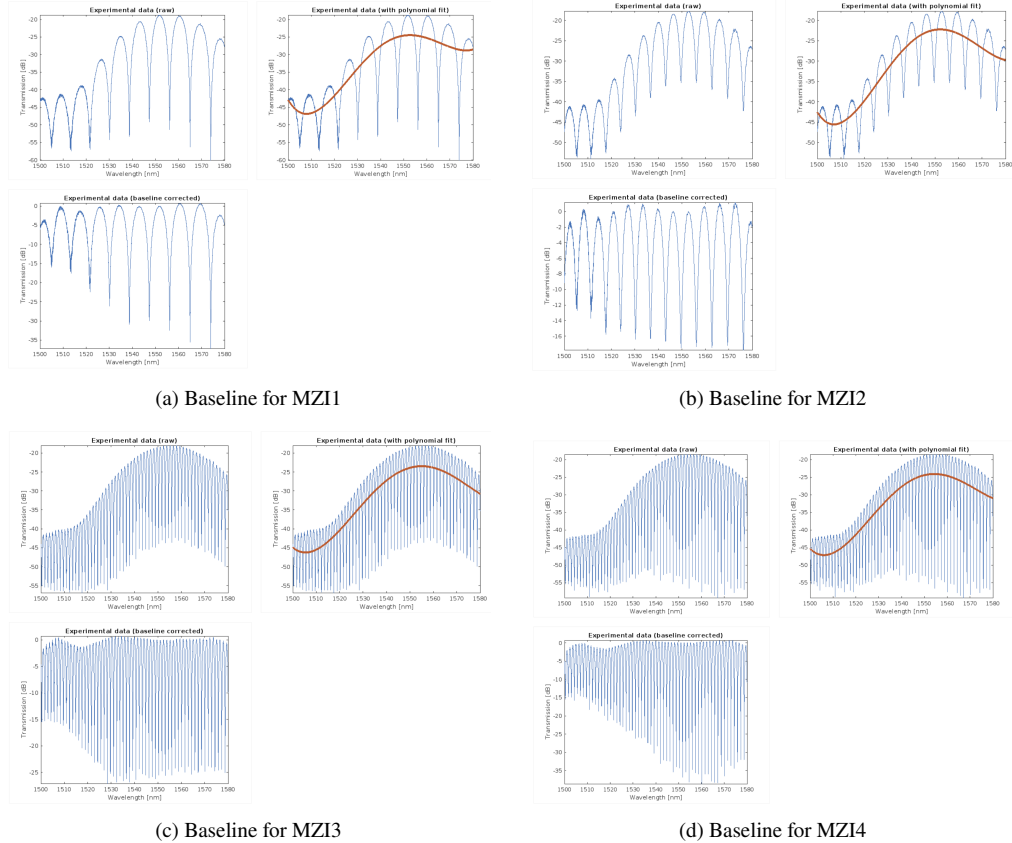


Fig. 4. Baseline responses for MZI1–MZI4.

48 4.2. Loopback Calibration

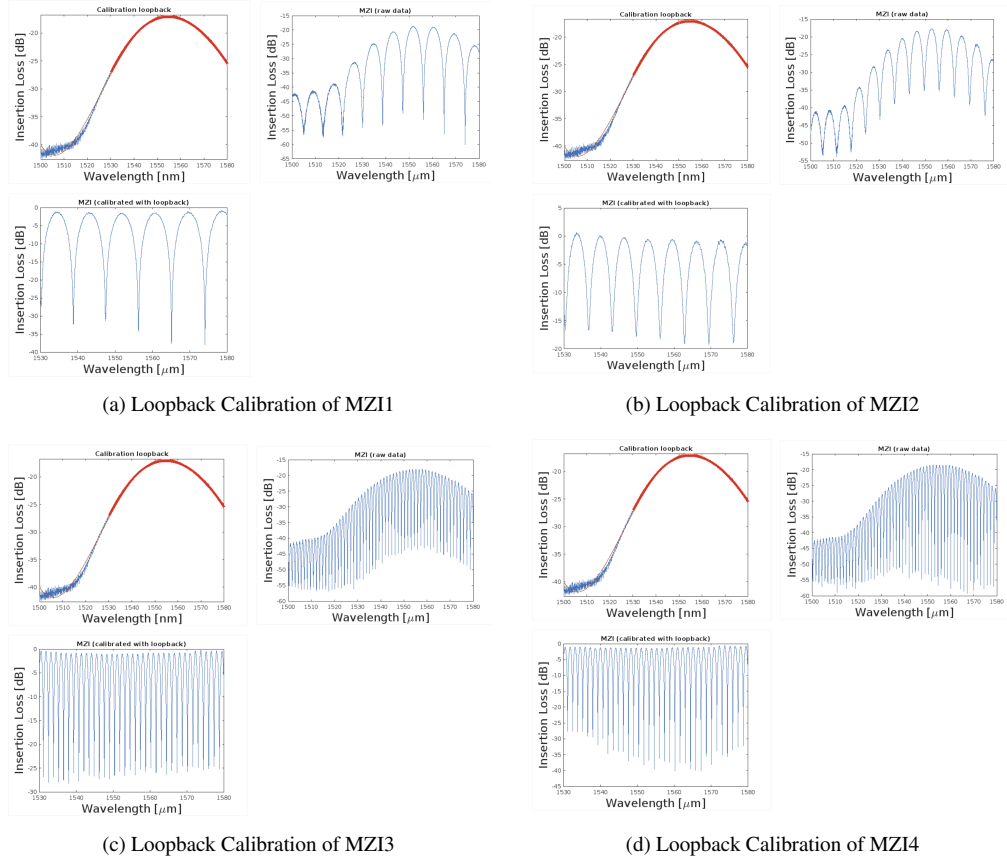


Fig. 5. Loopback Calibration for MZI1–MZI4.

49 4.3. Curve Fitting

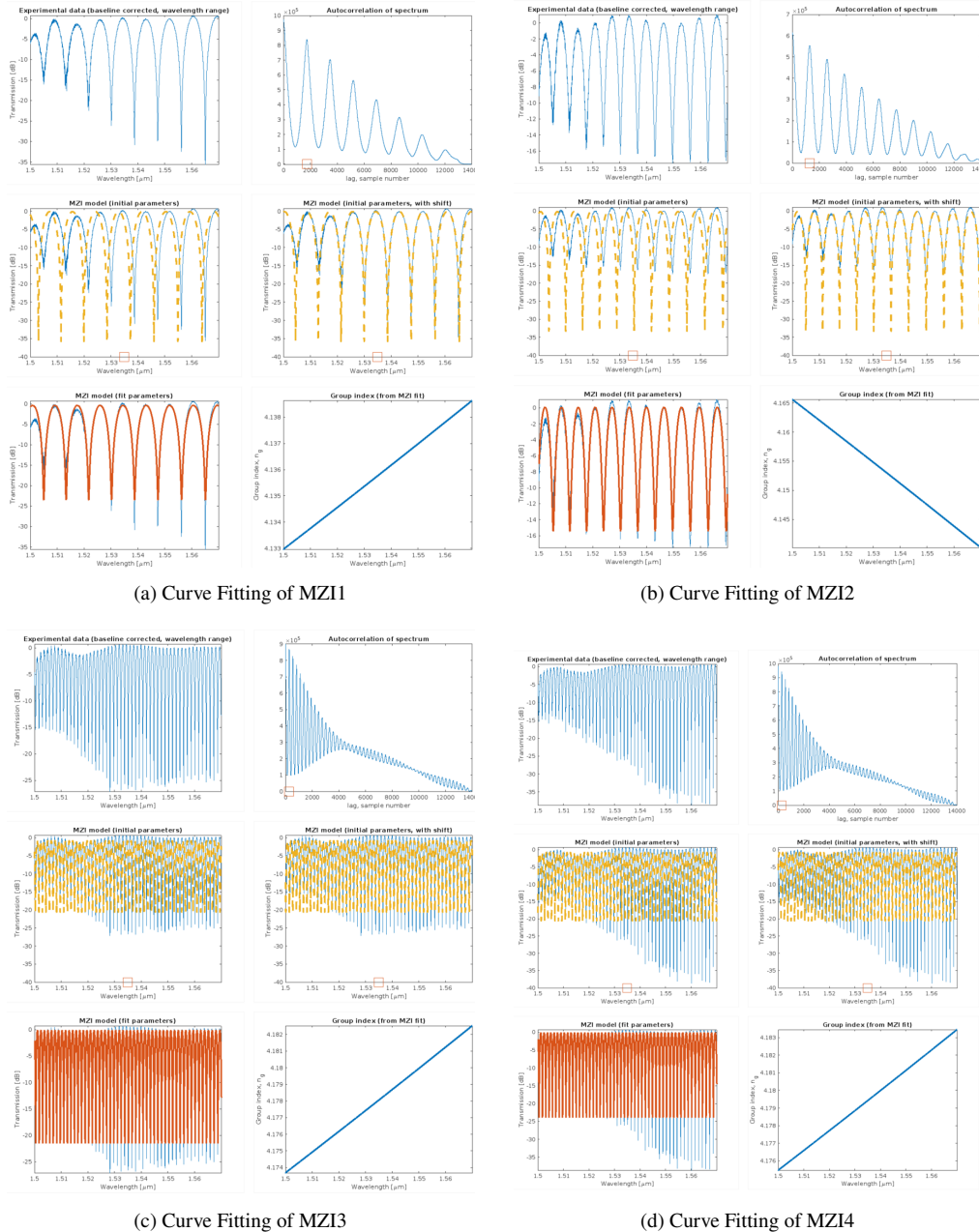


Fig. 6. Curve Fitting for MZI1–MZI4.

50 **References**